Dalton Transactions

Novel core-shell structure microspheres based on lanthanide complexes for white light emission and fluorescence sensing

Journal:	*Dalton Transactions*
Manuscript ID	DT-ART-10-2015-003939.R1
Article Type:	Paper
Date Submitted by the Author:	29-Nov-2015
Complete List of Authors:	Lian, Xiao; Tongji University Yan, Bing; Tongji University, Department of Chemistry

Journal Name

ARTICLE

Novel core-shell structure microspheres based on lanthanide complexes for white light emission and fluorescence sensing

Received 00th January 20xx,
Accepted 00th January 20xx

DOI: 10.1039/x0xx00000x

www.rsc.org/

Xiao Lian, Bing Yan

A series of new core-shell structure materials based on lanthanide complexes $[H_2NMe_2]_3[Ln(dpa)_3]$ (Ln = Eu, Tb, Sm, Dy, Nd, Yb; $[H_2NMe_2]^+$ = dimethyl amino cation; dpa = 2-dipicolinate) and silica microspheres are prepared under solvothermal conditions. Electron microscopy reveals that the nanosize materials SiO_2@Ln-dpa are spherical shaped with narrow size distribution and the $[H_2NMe_2]_3[Ln(L)_3]$ coating is generated on the surface of silica microspheres successfully. The core-shell structure materials exhibit excellent optical performance. The white light emitting material SiO_2@(Dy:Eu)-dpa reveals potential application to develop for white light device, as a result of its CIE chromaticity coordinate was very close to the pure white area. Then we selected the SiO_2@Eu-dpa as a representative sample for sensing experiment. Eventually, we find that the core-shell structure sensors reveal highly selective and sensitive for acetone and Cu^{2+} cations. The detection of Cu^{2+} in the human body is an important issue. Interestingly, the core-shell structure materials show better selectivity and higher sensitivity than the pure lanthanide complexes in Cu^{2+} sensing event, and the quenching effect coefficient value has increased more than twenty percent.

Introduction

Lanthanide hybrid materials have attracted great interest in the last twenty years, as they possess improved chemical stability, thermal stability and mechanical resistance.[1] Multifunctional hybrids or nanocomposites based on luminescent lanthanide complexes have seen a great interest both in fundamental research and practical application,[2] in which the thermal stability and mechanical properties of lanthanide complexes can be improved. In recent years, some novel lanthanide hybrid materials have been developed. Like lanthanide coordination polymers, also known as lanthanide metal–organic frameworks for those porous ones, have been rapidly growing as a new type of multi-functional materials in the last decades.[3]

The advantage of lanthanide inorganic–organic hybrid materials over other luminescent materials include that the combination with the organic and inorganic components, and the sharp and strong emissions, large Stokes shifts, high quantum yields and long luminescent lifetimes derive which originate from f-f transitions of lanthanide ions.[4] Therefore, they are expected to be promising luminescent dopants for the preparation of organic–inorganic hybrids with potential application in phosphors, solid-state lighting, integrated optics, optical telecommunications, solar cells, and biomedicine.[2a, 2c, 2d, 5] Among all the lanthanide hybrids, the derived silica host hybrids are the most popular, which is based on the functional bridge molecule (chemical linker) possessing three functions of coordinating/sensitizing lanthanide ions and sol–gel processing to constitute a covalent Si–O network.[6] Lanthanide ions species will covalently bonded Si–O network, which can solve the homogeneous dispersion and luminescent stability.

The efficient detection of small organic molecules and metal ions is important in many environmental and biological systems. Especially, the detection of Cu^{2+} in the human body is an essential issue in medicine, because Cu^{2+} plays considerable roles in living organisms.[7] A few lanthanide inorganic–organic hybrid materials reported have been constructed for Cu^{2+} sensing.[8] In recent years, the chemical sensors including discrete molecular chemical sensor systems and heterogeneous solid sensing has made great progress.[9] The heterogeneous solid sensors, including core-shell structure materials, which exhibit excellent chemical stability, low pollution, and recyclable potential, are a kind of promising sensor in practice. However, low sensitivity and weak signals are two problems need to be solved for heterogeneous solid sensors. Thus the development of highly effective solid sensor materials is still an important and challenging area. Many properties of nano-objects such as quantum size effect, and surface-enhanced Raman scattering are their size, shape and

Department of Chemistry, Tongji University, Siping Road 1239, Shanghai 200092, China. E-mail: byan@tongji.edu.cn
† Footnotes relating to the title and/or authors should appear here.
Electronic Supplementary Information (ESI) available: [details of any supplementary information available should be included here]. See DOI: 10.1039/x0xx00000x

composition related.[10] Novel strategy has been developed to synthesize core-shell structure lanthanide hybrid materials of encapsulating pre-synthesized nano-objects with the post-formation of shells on their surfaces.[11]

To date, several research groups have recently developed nano- and micro-sized lanthanide hybrid materials.[4b, 12, 13] In this work, we report a facile route for synthesis of core-shell structure microspheres based on silica and $[H_2NMe_2]_3[Ln(dpa)_3]$ (Ln = Eu, Tb, Sm, Dy, Nd, Yb; $[H_2NMe_2]^+$ = dimethyl amino cation; dpa = 2-dipicolinate). Nano-size silica sphere (with a diameter about 210 nm) belongs to a suitable substrate for fluorescence sensors due to the excellent stability and optical transparent. In addition, the uncomplicated implement to modify with –COOH group of silica and the inside of solid sensor materials are not important for the effective sensing process are also taking into consideration.[11a, 14] The core-shell structure materials SiO_2@Ln-dpa (Ln = Eu, Tb, Sm, Dy, Yb and Nd) display excellent optical properties for application in development of white light device, small organic molecule or Cu^{2+} sensor (See the scheme in Fig. 1).

Experimental section

Reagents and chemicals

All chemicals and solvents used were commercially available and at least of analytical grade. Lanthanide nitrates $Ln(NO_3)_3{\cdot}6H_2O$ (Ln = Eu, Tb, Sm, Dy, Nd, Yb) were prepared by dissolving their respective oxides in concentrated nitric acid with heating and stirring to promote the reaction. 3-Aminopropyltriethoxysilane (95 %, APTES), succinic anhydride (99 %) and 2,6-dipicolinic acid (99 %, 2,6-H_2dpa) were purchased from Adams. DMF solutions of Na^+, Ca^{2+}, Zn^{2+}, Ag^+, Cr^{3+}, Al^{3+}, Cu^{2+}, and Fe^{3+} were prepared from their respective nitrate salts; solutions of Cd^{2+} and Fe^{2+} were prepared from chlorate salts and Fe^{2+} solution was prepared immediately.

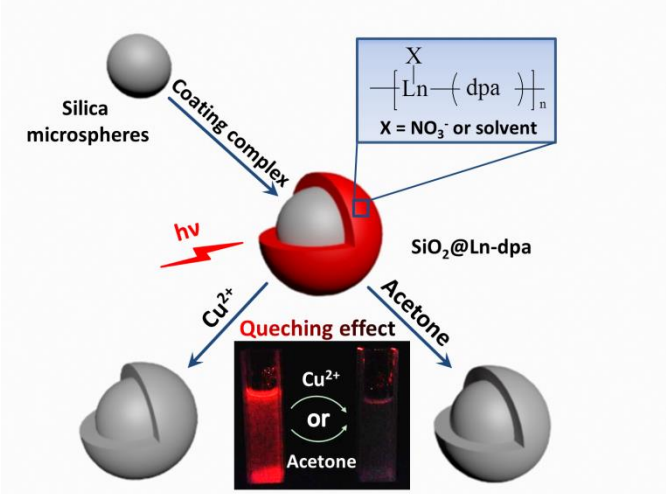

Fig. 1 Schematic diagram of synthesis and sensing process of SiO_2@Ln-dpa core-shell microspheres.

Instrumentation

The powder X-ray diffraction (PXRD) patterns were recorded with a Bruker Foucs D8 diffractometer using CuKα radiation with 40 mA and 40 kV. Fourier transform infrared spectra (FTIR) were recorded with KBr slices from 4000–400 cm^{-1} using a Nexus 912 AO446 infrared spectrophotometer. Raman spectra were carried out on a Laser Confocal Micro-Raman Spectrometer (Renishaw Invia). Fluorescence spectra were performed on an Edinburgh Analytical Instrument FLS920. Lifetime measurements were measured at an Edinburgh Instruments FLS920 fluorescence spectrometer using a microsecond (100 mW) lamp. The outer luminescent quantum efficiency was determined by an integrating sphere (150 mm diameter, $BaSO_4$ coating) on Edinburgh FLS920 spectrometer. This method has been widely used in determining quantum yields. Transmission electron microscopy (TEM) was carried on a JEOL JEM-2010F transmission electron microscope operating at 200 kV. Scanning electron microscopy (SEM) and energy dispersive analysis of X-rays (EDX) was performed on a Hitachi S-4800 field emission scanning electron microscope operating at 15 kV. The ultraviolet diffuse-reflectance spectra of the powdered samples were recorded by a B&W Tek BWS003 spectrophotometer.

Preparation of the carboxylate-functionalized silica microspheres

Bare silica spheres (200 nm) were obtained by using a conventional method. Carboxylate-functionalized silica microspheres were synthesized according to the previously reported literature. The silane coupling agent APTES (2.8 g, 0.012 mol) in dry THF (30 mL) was added dropwise to a solution of succinic anhydride (1.3 g, 0.013 mol) in dry THF (20mL). After stirring the mixture for 12 h at room temperature, a solution containing silica microspheres (2.0 g), THF (30 mL) and H_2O (6 mL) was added into the mixture. Continuous stirring at least six hours, the final products were separated from the reaction mixture by centrifugation and washed with methanol. After drying in vacuum, the carboxylate-functionalized silica microspheres were obtained.

Preparation of $[H_2NMe_2]_3[Ln(dpa)_3]$ (Ln = Eu, Tb, dpa = 2,6-dipicolinate)

$[H_2NMe_2]_3[Ln(dpa)_3]$ was synthesized according to Mooibroek *et al*.[15a] Typically, $Ln(NO_3)_3{\cdot}6H_2O$ (0.5 mmol) and 2,6-H_2dpa (0.3342 g, 2 mmol) were placed in a 50 mL bottle and dissolved in 14 mL mixed-solvent of DMF (12 mL) and H_2O (2 mL). The mixture was heated at 393 K for 72 h. The white powdered products were collected by centrifugation and then dried at 353 K for 6 h.

Preparation of the SiO_2@Ln-dpa core-shell microspheres

Firstly, $Ln(NO_3)_3{\cdot}6H_2O$ (0.5 mmol) and 2,6-H_2dpa (0.3342 g, 2 mmol) were dissolved in 12 mL DMF. Then, a suspension contained carboxylate-functionalized silica microspheres (0.6 g) and H_2O (2 mL) were added into the above mentioned solution with stirring. The mixture was heated further in a polytetrafluoroethylene (PTFE)-lined steel autoclave for the hydrothermal reaction for 72 h at 393 K. The solid products were collected via centrifugation. Finally, the products were

washed with methanol for several times, and then dried at 333 K for 6 h.

Luminescence sensing experiments

For small organic molecules sensing, SiO_2@Eu-dpa powders (4 mg) were simply immersed in diverse organic solvents (dichloromethane, chloroform, methanol, ethanol, ethylene glycol 1,2-dichloroethane, ether, acetonitrile, acetone, butyl alcohol, amyl alcohol, N,N-dimethylformamide (DMF) and tetrahydrofuran (THF)) at room temperature. For cations sensing, SiO_2@Eu-dpa powders (4 mg) were simply immersed in the DMF solutions of $M(NO_3)_z$ (10^{-3} M, 3 mL) at room temperature (M^{z+} = Na^+, Ca^{2+}, Zn^{2+}, Ag^+, Cr^{3+}, Al^{3+}, Cu^{2+}, Fe^{3+}, Cd^{2+} and Fe^{2+}). The mixtures were then sonicated for 5 min to prepare the metal ion-incorporated suspension for luminescent measurements.[16]

Result and discussion

Characterization of core-shell structure SiO_2@Ln-dpa hybrids

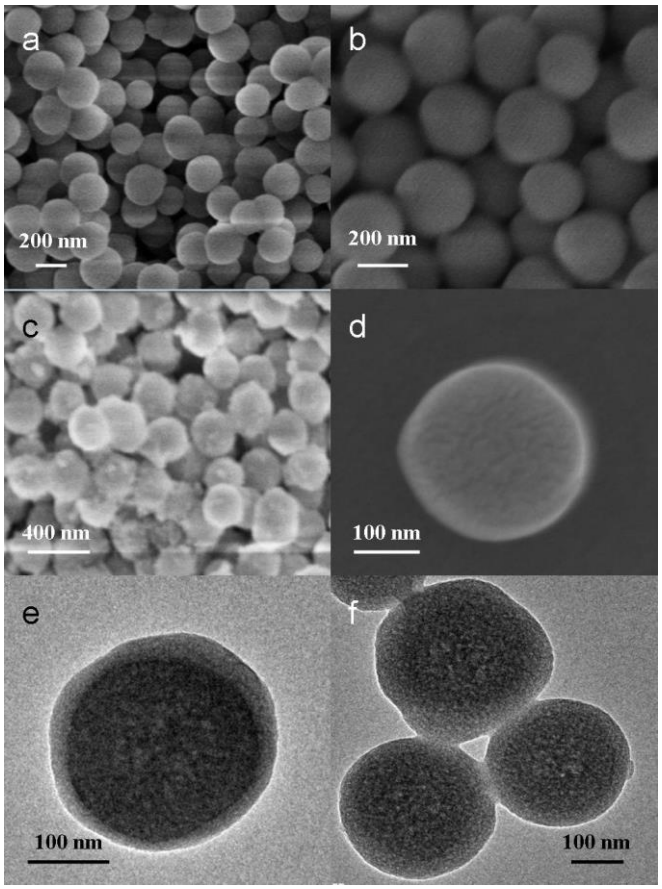

Fig. 2 (a-b) SEM images of carboxylate-terminated silica spheres with an average diameter of 210 ± 20 nm. (c-d) SEM and (e-f) TEM images of SiO_2@Ln-dpa core-shell microspheres with an average diameter of 270 ± 20 nm. The average diameters were measured from SEM images.

A series of materials of SiO_2@Ln-dpa (Ln = Eu, Tb, Sm, Dy, Yb, Nd) and SiO_2@(Eu:Tb)-dpa, SiO_2@(Dy:Eu)-dpa are hydrothermal synthesized.[15] The formation of monodisperse SiO_2@Ln-dpa core–shell micro-spheres are verified by scanning electron microscopy (SEM) and transmission electron microscopy (TEM), respectively (Fig. 2). The TEM images obviously validate the formation of the core–shell structure, as shown in Fig. 2e–f. The pale edges and the dark center are the typical feature for core–shell materials. The diameter change from 210 nm for the raw silica microspheres to 270 nm after the solvothermal reaction indicates that the generated complexes shells with thicknesses of about 30 nm surrounding the core (Fig. 2a-d). In addition, as we can infer from Fig. 2f, the border between the $[H_2NMe_2]_3[Ln(dpa)_3]$ shell and the SiO_2 core reveals to be indistinct, which is probably due to the slight mass difference of the two components. SEM images (Fig. 2c) demonstrate that SiO_2@Ln-dpa were spherical shaped with narrow size and the size distribution is shown in the Fig. S6. The composition of the resulting microspheres is subsequently analysed by energy dispersive analysis by X-rays (EDX) spectroscopy (Fig. S7). The existence of silicon atoms (1.09 %) in the EDX spectrum of these microspheres supports the formation of core-shell structure containing silicon atoms on the shells. The topological information of the resulting shell is obtained from the powder X-ray diffraction (PXRD) pattern (Fig. 3), which clearly shows the structure of SiO_2 which after coating the $[H_2NMe_2]_3[Ln(dpa)_3]$, in accordance with the PXRD patterns obtained from pure $[H_2NMe_2]_3[Ln(dpa)_3]$ crystals, as another evidence for the successful synthesis process.

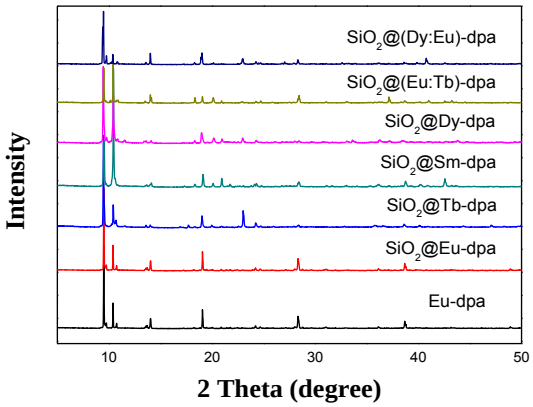

Fig. 3 PXRD patterns of Eu-dpa and SiO_2@Ln-dpa core-shell microspheres. The PXRD pattern of SiO_2@Ln-dpa exhibits several peaks in 2θ ranged 5-50 °, which matches well with the XRD pattern of pure $[H_2NMe_2]_3[Ln(dpa)_3]$.

To further prove the successful coating with $[H_2NMe_2]_3[Ln(dpa)_3]$, Fourier transform infrared spectra (FTIR) and Raman spectra are recorded for bare SiO_2, carboxylate-functionalized silica microspheres, $[H_2NMe_2]_3[Ln(dpa)_3]$ and SiO_2@Ln-dpa (Fig. 4, Fig. S8). Comparing to bare silica spheres, the increase of the peak intensity at 1101 cm^{-1} for Si-O-Si (ν_{as}) bond from the spectra of SiO_2-COOH certificates the combination of 3-aminopropyl-triethoxysilane (APTES) with the hydroxyl group on the surface of SiO_2, and the appearance of carboxyl characteristic peaks at 3000-3500 cm^{-1} and –CO-NH- at 1643 cm^{-1} also confirms the successful carboxyl modification of SiO_2. For the spectra of SiO_2@Ln-dpa core-shell materials, the appearance of the characteristic peaks of $[H_2NMe_2]_3[Ln(dpa)_3]$ indicates that its crystals form and grow

on the surface of the silica microspheres. Furthermore, the characteristic bands of Si-O at 800 cm^{-1} (ν_s) and 472 cm^{-1} (δ) for these three kinds of materials also demonstrate that the carboxyl modification and MOFs formation did not damage the chemical bonds and structure of the bare SiO_2. The characteristic peaks of Si-O-Si (vas, 1084 cm-1), Si-OH (vs, 961 cm-1), and Si-O (δ, 498 cm-1) from the Raman spectra of SiO_2@Ln-dpa are another proof for the successful preparation of core-shell structure (Fig. S8).

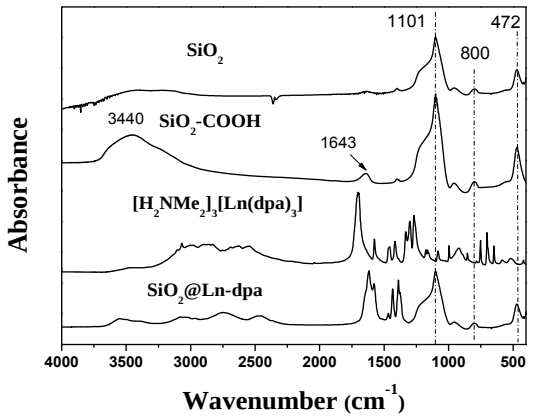

Fig. 4 FTIR spectra of bare SiO_2, SiO_2-COOH, $[H_2NMe_2]_3[Ln(dpa)_3]$ and SiO_2@Ln-dpa microspheres.

Luminescence properties of SiO_2@Ln-dpa

The fluorescence spectra of SiO_2@Ln-dpa microspheres show the characteristic transitions of lanthanide ions. Fig. 5a shows the excitation and emission spectra of SiO_2@Eu-dpa, whose emission bands at 594, 615, 651 and 695 nm are ascribed to the $^5D_0 \rightarrow {}^7F_J$ (J = 1, 2, 3, 4) transitions of Eu^{3+} ions respectively. The characteristic Tb^{3+} ion emission can be observed in Fig. 5b, which is assigned to the $^5D_4 \rightarrow {}^7F_J$ (J = 6, 5, 4, 3) transitions at 492, 545, 584 and 622 nm. The emission peaks of SiO_2@Sm-dpa are assigned to $^4G_{5/2} \rightarrow {}^6H_{J/2}$ (J = 5, 7, 9 and 11) transitions for the peaks located at 563, 603, 644 and 705 nm, respectively (Fig. S9). We can observe that the emission lines are assigned to $^4F_{9/2} \rightarrow {}^6F_{15/2}$ and $^4F_{9/2} \rightarrow {}^6F_{13/2}$ transitions for the peaks located at 482 and 573 nm from the spectra of SiO_2@Dy-dpa (Fig. S10). The CIE (Commission International de L'Eclairage) chromaticity diagram of these materials is illustrated in Fig. S11. For SiO_2@Yb-dpa and SiO_2@Nd-dpa, the emission bands at 981 nm in Fig. 5c and 1061 nm in the Fig. 5d are attributed to the $^2F_{5/2} \rightarrow {}^2F_{7/2}$ transition of Yb^{3+} ions and $^4F_{3/2} \rightarrow {}^4I_{11/2}$ transition of Nd^{3+} ions separately. It is clearly shown that all the excitation spectra (the black line) are dominated by broad absorption bands located in the ultraviolet region centered at about 300 nm, suggesting that the resulting materials can absorb the ultraviolet light efficiently and then sensitize the emission of lanthanides by energy transfer. This is owing to the same sensitizing ligand, 2,6-H_2dpa. This endows SiO_2@Ln-dpa core-shell materials with the same maximum excitation wavelength, whatever the lanthanide ion is.[17]

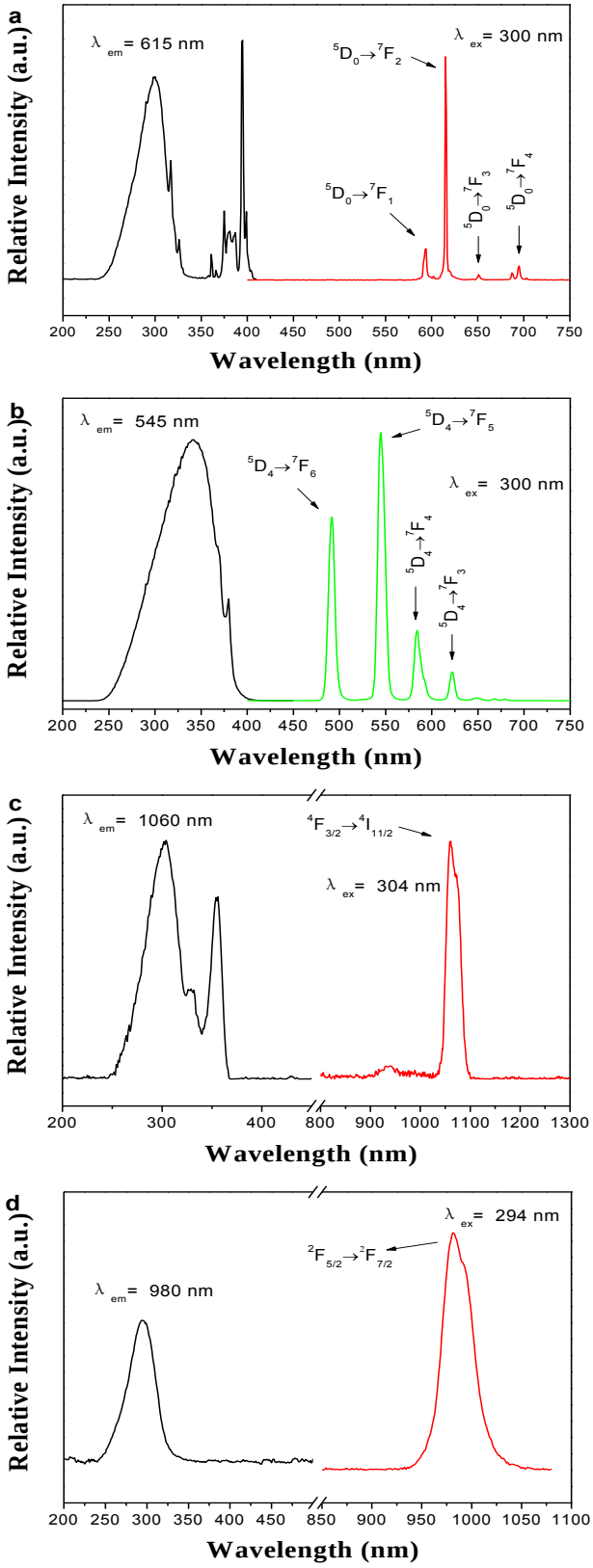

Fig. 5 Fluorescence spectra of as-synthesized (a) SiO_2@Eu-dpa; (b) SiO_2@Tb- dpa; (c) SiO_2@Yb-dpa and (d) SiO_2@Nd-dpa.

To further study the luminescence performance of these core-shell materials and $[H_2NMe_2]_3[Ln(dpa)_3]$, their typical decay curves and the luminescent lifetimes for dominant emissive Eu^{3+} ($^5D_0 \rightarrow {}^7F_2$) and Tb^{3+} ($^5D_4 \rightarrow {}^7F_5$) are measured. The resulting data of these materials are listed in Table. S1. It can be observed that the total quantum yield of SiO_2@Eu-dpa were longer than SiO_2@Tb-dpa. This is probably for the fact that the energy match between 2,6-dpa and Eu^{3+} is more effective than Tb^{3+}.[18] In addition, according to the reported literature,[15] the lifetimes and total quantum yield are higher than which of ours. For this phenomenon, we think that the species and contents of lanthanide ions of the complexes Ln-H2dpa, the purity of raw materials, the details of synthesis process and the conditions of luminescence experiments are the possible reasons. But in our research, the lifetimes and total quantum yield of SiO_2@Ln-dpa are much better than the corresponding pure lanthanide complexes, which indicated the core-shell materials has better application potential such as optical device and chemical sensing.

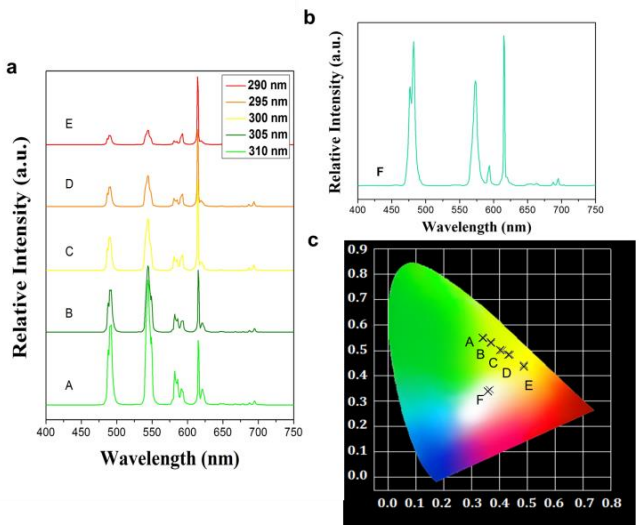

Fig. 6 (a) Fluorescence spectra of SiO_2@(Eu:Tb)-dpa excited from 290 nm to 310 nm; (b) fluorescence spectra of SiO_2@(Dy:Eu)-dpa; (c) CIE chromaticity diagram.

Sensing for small organic molecules

To examine the potential of the SiO_2@Eu-dpa for the sensing of small organic molecules, the material is immersed in different organic solvents (dichloromethane, chloroform, methanol, ethanol, ethylene glycol 1,2-dichloroethane, ether, acetonitrile, acetone, butyl alcohol, amyl alcohol, DMF and THF) for luminescence studies. As shown in Fig. 7, the emission intensities of SiO_2@Eu-dpa from $^5D_0 \rightarrow {}^7F_2$ transition of Eu^{3+} in the emission spectra are strongly influenced by the solvent, especially in the case of acetone, which exhibits the most significant quenching effects. Fig. 8 shows the emission spectrum of SiO_2@Eu-dpa dispersed in acetone-DMF mixed solvent with different volume ratio ($V_{acetone}/V_{DMF}$). The fluorescence intensity of the SiO_2@Eu-dpa suspension gradually decreases with the increase of the content of acetone, and almost disappeared at an acetone content of 5.0 Vol%. This decreasing tendency of the luminescence intensity derived from the quenching effect of acetone may be significant to detect the presence of acetone in solution. It is noting that all measurements are treated with ultrasonic interaction above 5 minutes after adding solvents and the excited wavelength was 300 nm.

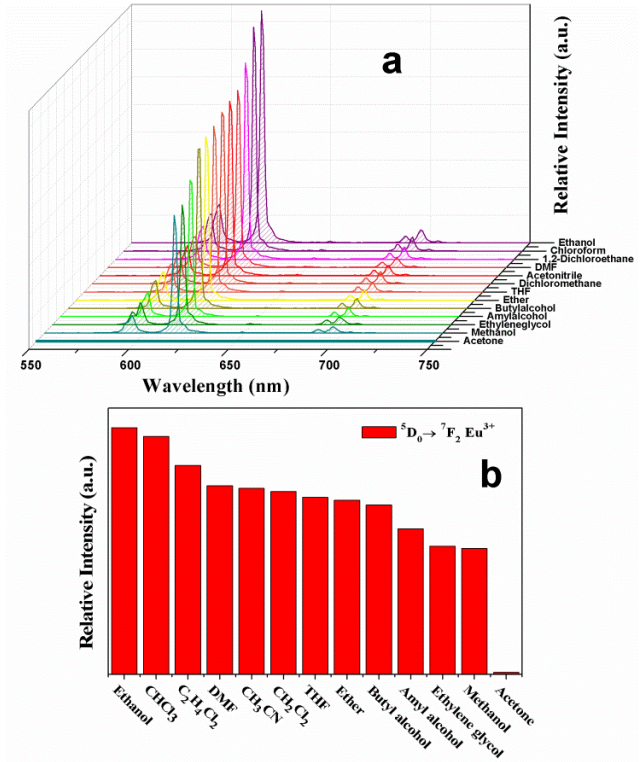

Fig. 7 (a) Fluorescence spectrum intensity and (b) the $^5D_0 \rightarrow {}^7F_2$ transition intensities of SiO_2@Eu-dpa introduced into various pure solvents when excited at 300 nm.

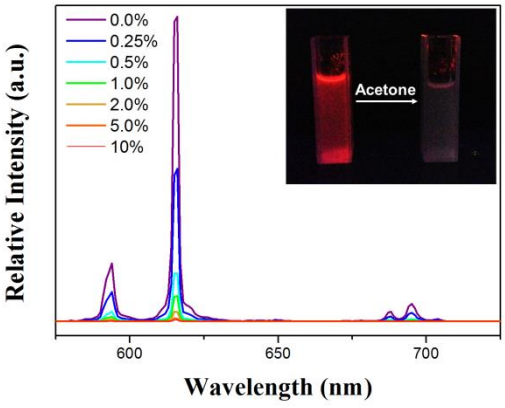

Fig. 8 The emission spectra of SiO_2@Eu-dpa dispersed in different content acetone-DMF mixed solvent. The inset shows the luminescence change after the addition of acetone in SiO_2@Eu-dpa suspension under UV light.

In order to investigate the mechanism of this quenching phenomenon, the UV–vis absorption spectroscopy of acetone as well as ultraviolet diffuse-reflectance spectra of 2,6-H_2dpa and SiO_2@Eu-dpa are performed (Fig. S12). The strong absorption band of dpa is located from 280 to 520 nm and the maximum absorption wavelength is above 360 nm that is largely overlapped by the absorbing band of acetone (250-400

nm). According to the absorption and luminescent spectra, it is suggested that there is a competition of the absorption of the excited energy between dpa and acetone, which affects the energy transfer between dpa and Eu^{3+} (antenna effect) to produce the weakening or even quenching effect of fluorescent intensity. The quenching mechanism is also in accordance with reported literature.[8b, 20]

Luminescent sensing for Cu^{2+}

The utilization of SiO_2@Eu-dpa core-shell materials as a luminescent sensor for metal ion detection is then investigated. The as-synthesized SiO_2@Eu-dpa is immersed in DMF solutions containing various cations (Na^+, Ca^{2+}, Cu^{2+}, Zn^{2+}, Cd^{2+}, Fe^{2+}, Fe^{3+}, Cr^{3+}, Al^{3+} and Ag^+) to form stable suspensions for luminescence studies. These metal cations include the macroelements (Na^+, Ca^{2+}), trace elements (Fe^{2+}, Fe^{3+}, Cu^{2+}, Zn^{2+}, Cr^{3+}) and some potentially toxic or benefit elements (Cd^{2+}, Al^{3+}, Ag^+) for human body. The luminescent spectra and histogram are shown in Fig. 9. It is can be observed that lots of kinds of metal cations caused attenuation of the fluorescence intensity of SiO_2@Eu-dpa originated from $^5D_0 \rightarrow {}^7F_2$ transition of Eu^{3+}. However, only Cu^{2+} reveals a conspicuous quenching effect on the luminescence originated from the f-f transition of Eu^{3+}.

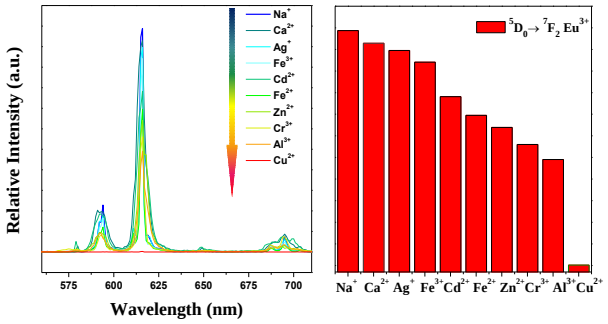

Fig. 9 Responses of the fluorescence of SiO_2@Eu-dpa towards DMF solution of various metal cations (5 mM). All of the emission spectra were collected at the excitation wavelength of 300 nm.

For the purpose of understanding the response of fluorescence of SiO_2@Eu-dpa for Cu^{2+} cations, the luminescence titration upon the addition of the solution that $Cu(NO_3)_2$ dissolved in DMF to SiO_2@Eu-dpa were further executed. The well-dispersed DMF suspensions of the core-shell microspheres with various concentrations of Cu^{2+} exhibited a decrease of the luminescence intensity of SiO_2@Eu-dpa microspheres with increasing contents of Cu^{2+} from 0 to 500μM (Fig. 10a). The luminescent turn-off effect on Cu^{2+} of SiO_2@Eu-dpa is also easily observed by the naked eye, as shown in Fig. S13. In addition, we also compared the sensitivity of different sensing materials with silica cores or without cores for Cu^{2+} detection. As demonstrated in Fig. 10b, the quenching effect coefficient K_{sv} value (2.93×10^4 M^{-1}) of core-shell materials exhibit more than 20% improvement over the pure Eu-dpa complex (2.29×10^4 M^{-1}). The quantified value of the quenching effect of Cu^{2+} is obtained using the Stern-Volmer equation ($I_0/I = 1 + K_{sv} \times [M]$), where [M] is the concentration of Cu^{2+} and the values I_0 and I are the luminescence intensity of the materials suspension without and with addition of Cu^{2+}, respectively. This result indicates that the core-shell structure materials display better selectivity and higher sensitivity than the pure Ln-Dpa and another Cu^{2+} sensor based on lanthanide complexes which have been reported.[21]

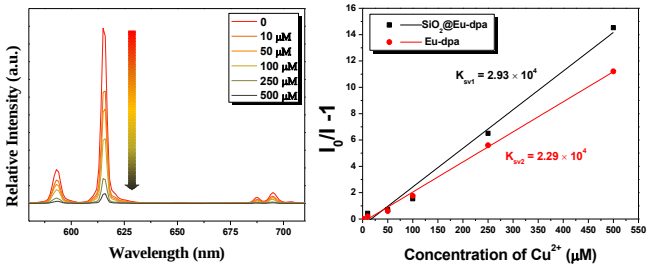

Fig. 10 Emission spectra of SiO_2@Eu-dpa (a) and linear fitting curve of the luminescence intensity of SiO_2@Eu-dpa (black) and pure Eu-dpa complex (red) (b) in DMF suspensions in the presence of various concentrations of Cu^{2+} under excitation at 285 nm.

Furthermore, we investigate the possible mechanism for such luminescence quenching effect of metal cations. It has been reported that the quenching effect on luminescence of lanthanide complexes by metal cations originates from three approaches: (1) the interaction between metal cations and organic ligands;[8a, 22] (2) the collapse of the crystal structure by metal cations;[23] (3) the cation exchange of central cations in the framework with cations.[9c, 24] To expound the possible sensing mechanism for luminescence quenching effect from the metal ions, FTIR and PXRD are employed to study the structural data of the SiO_2@Eu-dpa which were after the Cu^{2+} sensing experiment. Fig. S14 shows the information of the structure and chemical bonds of the core-shell materials which soaked in DMF solution contained Cu^{2+} for 2h. It is clear that the crystallinity of the materials changes markedly compared to Fig. 3 and the PXRD pattern reveals that the structure of the treated core-shell materials turns into amorphous. The FTIR spectra indicate that the information of characteristic bonds of the treated materials consistent with SiO_2-COOH (Fig. S14a). This result suggests that the crystal structure changes and collapsed. Hence, this selective sensitization of Cu^{2+} is realized due to the complete destruction of the original crystal framework which causes by copper ions and leads to the luminescence of Eu^{3+} disappears completely.

Here it is worthy pointing out that we only preliminarily check its sensing property of Cu^{2+} in DMF solutions in this work. Much effort needs to be done to check the sensing and stability of these hybrid materials in aqueous solution for biological application. So the future work should be studied deeply to explore the practicability.

Conclusion

In summary, we have successfully synthesized a core-shell structure microspheres by the growth of a $[H_2NMe_2]_3[Ln(dpa)_3]$ shell on spherical carboxylate terminated SiO_2 cores via easily

hydrothermal synthesis. The small size (280 ± 10 nm) and excellent luminous performance of SiO_2@Ln-dpa microspheres make it possible for optical device and selective sensors. Under the excitation of ultraviolet light, several kinds of materials adulterated different lanthanide ions display their characteristic emission spectrum. Moreover, the core-shell materials containing different kinds of lanthanide ions reveal the potential application that develops to the white light device. Interestingly, SiO_2@Eu-dpa microspheres are sufficient for a reliable sensing process for acetone and Cu^{2+}. In addition, the mechanism of the quenching effect is investigated on both of acetone and Cu^{2+}. It is expected that the easily obtained luminescent core-shell structure materials will likely develop become practical and useful sensors for detecting small organic molecules and metal ions. This study provides the possibility for the preparation of multifunctional lanthanide complexes based composites for wide applications.

Acknowledgements

This work was supported by the National Natural Science Foundation of China (21571142) and the Developing Science Funds of Tongji University (1380219059).

Notes and references

1. (*a*) K. Binnemans, *Chem. Rev.*, 2009, **109**, 4283; (*b*) C. Molina, R. A. S. Ferreira, G. Poirier, L. S. Fu, S. J. L. Ribeiro, Y. Messsaddeq and L. D. Carlos, *J. Phys. Chem. C*, 2008, **112**, 19346; (*c*) B. Yan, *RSC Advances*, 2012, **2**, 9304; (*d*) L. Guo, L. Fu, R. A. S. Ferreira, L. D. Carlos, Q. Li and B. Yan, *J. Mater. Chem.*, 2011, **21**, 15600; (*e*) B. H. Kwon, H. S. Jang, H. S. Yoo, S. W. Kim, D. S. Kang, S. Maeng, D. S. Jang, H. Kim and D. Y. Jeon, *J. Mater. Chem.*, 2011, **21**, 12812.
2. (*a*) L. D. Carlos, R. A. Ferreira, Z. Bermudez Vde and S. J. Ribeiro, *Adv. Mater.*, 2009, **21**, 509; (*b*) W. Rong, D. He, M. Wang, Z. Mou, J. Cheng, C. Yao, S. Li, A. A. Trifonov, D. M. Lyubov and D. Cui, *Chem. Commun.*, 2015, **51**, 5063; (*c*) S. F. H. Correia, V. D. Bermudez, S. J. L. Ribeiro, P. S. Andre, R. A. S. Ferreira and L. D. Carlos, *J. Mater. Chem. A*, 2014, **2**, 5580; (*d*) S. V. Eliseeva and J. C. G. Bunzli, *Chem. Soc. Rev.*, 2010, **39**, 189.
3. (*a*) Y. Han, X. Li, L. Li, C. Ma, Z. Shen, Y. Song and X. You, *Inorg. Chem.*, 2010, **49**, 10781; (*b*) B. Li, H.-M. Wen, Y. Cui, G. Qian and B. Chen, *Prog. Polym. Sci.*, 2015, **48**, 40; (*c*) Y. Cui, B. Chen and G. Qian, *Coordin. Chem. Rev.*, 2014, **273-274**, 76; (*d*) Y. Lu and B. Yan, *Chem. Commun.*, 2014, **50**, 15443.
4. (*a*) J. Rocha, L. D. Carlos, F. A. Paz and D. Ananias, *Chem. Soc. Rev.*, 2011, **40**, 926; (*b*) X. Zhang, W. Wang, Z. Hu, G. Wang and K. Uvdal, *Coordin. Chem. Rev.*, 2015, **284**, 206; (*c*) J. C. G. Bunzli, *Acc. Chem. Res.*, 2006, **39**, 53.
5. (*a*) A. N. Kuda-Wedagedara, C. Wang, P. D. Martin and M. J. Allen, *J. Am. Chem. Soc.*, 2015, **137**, 4960; (*b*) W. Y. Wong and C. L. Ho, *Acc. Chem. Res.*, 2010, **43**, 1246; (*c*) L. N. Sun, H. J. Zhang, L. S. Fu, F. Y. Liu, Q. G. Meng, C. Y. Peng and J. B. Yu, *Adv. Funct. Mater.*, 2005, **15**, 1041.
6. (*a*) H. R. Li, J. Lin, H. J. Zhang, H. C. Li, L. S. Fu and Q. G. Meng, *Chem. Commun.*, 2001, 1212; (*b*) D. Ananias, F. A. Paz, D. S. Yufit, L. D. Carlos and J. Rocha, *J. Am. Chem. Soc.*, 2015, **137**, 3051; (*c*) X. F. Qiao and B. Yan, *Inorg. Chem.*, 2009, **48**, 4714; (*d*) B. Yan and Y. F. Shao, *Dalton Trans.*, 2013, **42**, 9565.
7. (*a*) P. Gourdon, X. Y. Liu, T. Skjorringe, J. P. Morth, L. B. Moller, B. P. Pedersen and P. Nissen, *Nature*, 2011, **475**, 59; (*b*) I. Singh, A. P. Sagare, M. Coma, D. Perlmutter, R. Gelein, R. D. Bell, R. J. Deane, E. Zhong, M. Parisi, J. Ciszewski, R. T. Kasper and R. Deane, *PNAS*, 2013, **110**, 14771; (*c*) D. J. Waggoner, T. B. Bartnikas and J. D. Gitlin, *Neurobiol. Dis.*, 1999, **6**, 221.
8. (*a*) B. Chen, L. Wang, Y. Xiao, F. R. Fronczek, M. Xue, Y. Cui and G. Qian, *Angew. Chem. Int. Ed.*, 2009, **48**, 500; (*b*) Z. Hao, X. Song, M. Zhu, X. Meng, S. Zhao, S. Su, W. Yang, S. Song and H. Zhang, *J. Mater. Chem. A*, 2013, **1**, 11043; (*c*) S. Bhattacharyya, A. Chakraborty, K. Jayaramulu, A. Hazra and T. K. Maji, *Chem. Commun.*, 2014, **50**, 13567.
9. (*a*) W. Cho, H. J. Lee, S. Choi, Y. Kim and M. Oh, *Sci. Rep.*, 2014, **4**, 6518; (*b*) L. Mu, W. Shi, J. C. Chang and S. -T. Lee, *Nano Lett.*, 2008, **8**, 104; (*c*) Y. Zhou, H.-H. Chen and B. Yan, *J. Mater. Chem. A*, 2014, **2**, 13691; (*d*) N. Zhang, B. Zhu, F. Peng, X. Yu, Y. Jia, J. Wang, L. Kong, Z. Jin, T. Luo and J. Liu, *Chem. Commun.*, 2014, **50**, 7686; (*e*) J. Brunner and R. Kraemer, *J. Am. Chem. Soc.*, 2004, **126**, 13626.
10. S. Li and F. Huo, *Nanoscale*, 2015, **7**, 7482.
11. (*a*) H. Li, Q. Qin, L. Qiao, X. Shi and G. Xu, *Chem. Commun.*, 2015, **51**, 11321; (*b*) L. Wang, W. Yang, Y. Li, Z. Xie, W. Zhu and Z. M. Sun, *Chem. Commun.*, 2014, **50**, 11653; (*c*) Y. Wei, S. Han, D. A. Walker, P. E. Fuller and B. A. Grzybowski, *Angew. Chem. Int. Ed.*, 2012, **51**, 7435.
12. (*a*) R. Haldar, R. Matsuda, S. Kitagawa, S. J. George and T. K. Maji, *Angew. Chem. Int. Ed.*, 2014, **53**, 11772; (*b*) S. Furukawa, J. Reboul, S. Diring, K. Sumida and S. Kitagawa, *Chem. Soc. Rev.*, 2014, **43**, 5700; (*c*) C. M. Doherty, D. Buso, A. J. Hill, S. Furukawa, S. Kitagawa and P. Falcaro, *Acc. Chem. Res.*, 2014, **47**, 396.
13. J. L. Vivero-Escoto, R. C. Huxford-Phillips and W. Lin, *Chem. Soc. Rev.*, 2012, **41**, 2673.
14. (*a*) C. Jo, H. J. Lee and M. Oh, *Adv. Mater.*, 2011, **23**, 1716; (*b*) S. Sorribas, B. Zornoza, C. Tellez and J. Coronas, *Chem. Commun.*, 2012, **48**, 9388; (*c*) A. Ahmed, M. Forster, R. Clowes, D. Bradshaw, P. Myers and H. Zhang, *J. Mater. Chem. A*, 2013, **1**, 3276; (*d*) S. L. C. Pinho, S. Laurent, J. Rocha, A. Roch, M.-H. Delville, S. Mornet, L. D. Carlos, L. Vander Elst, R. N. Muller and C. F. G. C. Geraldes, *J. Phys. Chem. C*, 2012, **116**, 2285; (*e*) Y. Y. Fu, C. X. Yang and X. P. Yan, *Chem. Eur. J*, 2013, **19**, 13484.
15. (*a*) T. J. Mooibroek, P. Gamez, A. Pevec, M. Kasunic, B. Kozlevcar, W. T. Fu and J. Reedijk, *Dalton Trans.*, 2010, **39**, 6483; (*b*) H. Zhang, X. Shan, L. Zhou, P. Lin, R. Li, E. Ma, X. Guo and S. Du, *J. Mater. Chem. C*, 2013, **1**, 888.
16. J.-N. Hao and B. Yan, *J. Mater. Chem. C*, 2014, **2**, 6758.
17. Y. Lu and B. Yan, *J. Mater. Chem. C*, 2014, **2**, 5526.
18. L. Chen and B. Yan, *Dalton Trans.*, 2014, **43**, 14123.
19. X. Lian and B. Yan, *New J. Chem.*, 2015, **39**, 5898.
20. Y. Xiao, L. Wang, Y. Cui, B. Chen, F. Zapata and G. Qian, *J. Alloy. Compd.*, 2009, **484**, 601.
21. (*a*) Y. Q. Xiao, Y. J. Cui, Q. A. Zheng, S. C. Xiang, G. D. Qian and B. L. Chen, *Chem. Commun.*, 2010, **46**, 5503; (*b*) Z. M. Hao, G. C. Yang, X. Z. Song, M. Zhu, X. Meng, S. N. Zhao, S. Y. Song and H. J. Zhang, *J. Mater. Chem. A*, 2014, **2**, 237; (*c*) B. L. Chen, L. B. Wang, Y. Q. Xiao, F. R. Fronczek, M. Xue, Y. J. Cui and G. D. Qian, *Angew. Chem. Int. Ed.*, 2009, **48**, 500; (*d*) Z. M. Hao, X. Z. Song, M. Zhu, X. Meng, S. N. Zhao, S. Q. Su, W. T. Yang, S. Y. Song and H. J. Zhang, *J. Mater. Chem. A*, 2013, **1**, 11043.
22. Q. Tang, S. Liu, Y. Liu, J. Miao, S. Li, L. Zhang, Z. Shi and Z. Zheng, *Inorg. Chem.*, 2013, **52**, 2799.
23. S. Dang, E. Ma, Z.-M. Sun and H. Zhang, *J. Mater. Chem.*, 2012, **22**, 16920.
24. (*a*) C. X. Yang, H. B. Ren and X. P. Yan, *Anal. Chem.*, 2013, **85**, 7441; (*b*) M. Kim, J. F. Cahill, H. Fei, K. A. Prather and S. M. Cohen, *J. Am. Chem. Soc.*, 2012, **134**, 18082.

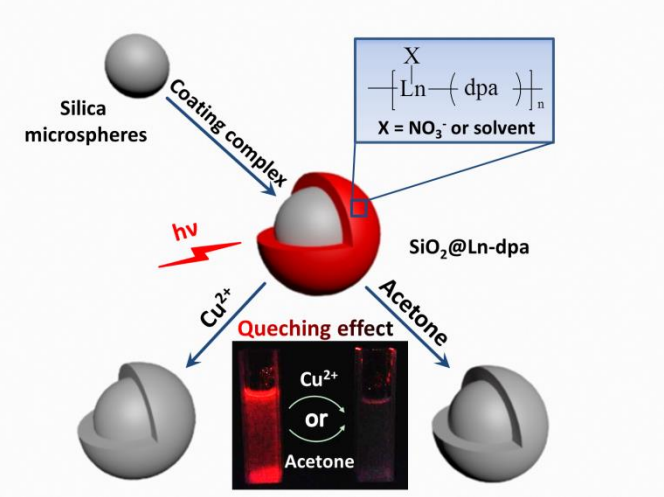

A series of new core-shell sturcture materials based on Ln-dpa complex and silica microspheres are prepared with narrow size distribution and the complex coating are generated on the surface of silica microspheres successfully. Among SiO_2@Dy:Eu-dpa exhibits white color luminescence. Furtherly SiO_2@Eu-dpa possesses highly selective and sensitive for acetone and Cu^{2+} cations, better than pure Ln-dpa complex in Cu^{2+}.